(T. L. Poulos, J. C. Vickery, H. Li in *Cytochrome P450: Structure, Mechanisms and Biochemistry*, 2nd ed. (Ed.: P. R. Ortiz de Montellano), Plenum, New York, **1995**, chap. 6). This will further make the donor ability of the cysteinato ligand similar to HS^-; b) both CPO and iNOS are known to possess more extensive hydrogen bonding to the cysteinato ligand and thereby weaken its interaction with the iron (D. L. Wang, D. J. Stuer, D. L. Rousseau, *Biochemistry* **1997**, *36*, 4595). In iNOS there is aromatic stacking which may stabilize the A_{2u} states with a prominent porphyrin hole (B. R. Crane, A. S. Arvai, R. Gacuchhui, C. Wu, D. Ghosh, E. D. Getzhoff, D. J. Stuehr, J. A. Tainer, *Science* **1997**, *278*, 425); c) for related discussions, see: H. Aissaoui, R. Bachmann, A. Schweiger, W.-D. Woggon, *Angew. Chem.* **1998**, *110*, 3191; *Angew. Chem. Int. Ed.* **1998**, *37*, 2998; D.Harris, G. H. Loew, *J. Am. Chem. Soc.* **1993**, *115*, 8775; d) to mimic the electric potential at the thiolate site, one needs electropositive moieties in model systems. See: H.-A. Wagenknecht, C. Claude, W.-D. Woggon, *Helv. Chim. Acta* **1998** *81*, 1506; e) for recent mutation that probe the distal and proximal pockets, see: M. P. Roach, A. E. Pond, M. R. Thomas, S. G. Boxer, J. H. Dawson, *J. Am. Chem. Soc.* **1999**, *121*, 12088; f) NH–S hydrogen bonding shortens the Fe–S bond in a synthetic model. See: N. Suzuki, T. Higuchi, Y. Urano, K. Kikuchi, H. Uekusa, Y. Ohashi, T. Uchida, T. Kitagawa, T. Nagano, *J. Am. Chem. Soc.* **1999**, *121*, 11571.

[13] E. D. Glendening, J. Badenhoop, A. E. Reed, J. E. Carpenter, F. Weinhold, Theoretical Chemistry Institute, University of Wisconsin, Madison, USA (NBO v.4.0). The natural orbital analysis identifies the three singly occupied orbitals (Scheme 2) and facilitates the states identification relative to the more tedious analysis of the UKS orbitals.

[14] J is evaluated using the formulae ($\boldsymbol{H}_{spin} = -J\boldsymbol{S}_1\boldsymbol{S}_2$), given in L. Noodleman, D. A. Case, *Adv. Inorg. Chem.* **1992** *38*, 423.

[15] For example, with basis set B1, the C_1 geometric parameters of the $^4A_{2u}$ ($^2A_{2u}$) states for **2a** are $r_{FeO} = 1.651$ (1.648), $r_{FeS} = 2.581$ (2.600), and $\Delta = 0.143$ (0.154) Å. The $^4A_{2u}$ ($^2A_{2u}$) energy difference is $+0.09$ kcal mol^{-1}. The main deviation from C_s symmetry is a tilt of the Fe–S axis off the C_s plane of symmetry and the energy stabilization of C_1 relative to C_s is small <1 kcal mol^{-1}.

[16] W. T. Borden in *Encyclopedia of Computational Chemistry*, *Vol. 1* (Eds.: P. von R. Schleyer, N. L. Allinger, T. Clark, J. Gasteiger, P. A. Kollman, H. F. Schaefer III, P. R. Schreiner), Wiley, Chichester, **1998**, p. 708.

[17] a) In the low-spin situation, the two natural orbitals form bonding and antibonding combinations; b) In C_1 some $A_{2u} - A_{1u}$ admixture is also expected. The A_{2u} parenthood is still apparent though in the calculation and the corresponding A_{1u} states are slightly higher in energy than the Π_S states; c) The perpendicular relation of the $p_\sigma(S)$ and $p_\pi(S)$ orbitals provides significant one center contribution to spin orbit coupling (SOC). A simple perturbation treatment of SOC ($\zeta_S = 388$ cm^{-1} and an energy gap taken from Figure 1) leads to a mixing coefficient of 0.14–0.18 from the quartet into the doublet state.

[18] N. Harris, S. Cohen, M. Filatov, F. Ogliaro, S. Shaik, *Angew. Chem.* **200**, *112*, 2070; *Angew. Chem. Int. Ed.* **2000**, *39*, 2003.

Formation of Novel Ordered Mesoporous Silicas with Square Channels and Their Direct Observation by Transmission Electron Microscopy**

Tatsuo Kimura, Takayuki Kamata, Minekazu Fuziwara, Yuri Takano, Mizue Kaneda, Yasuhiro Sakamoto, Osamu Terasaki, Yoshiyuki Sugahara, and Kazuyuki Kuroda*

Since the discovery of an ordered mesoporous silica,[1] the preparation of various mesoporous silicas by using surfactant assemblies has been developed.[2–4] These mesoporous silicas have proved to be highly applicable as catalysts, catalyst supports, and adsorbents for relatively large molecules,[5] which has stimulated a number of studies including both morphological control[6, 7] and compositional variations.[3, 8, 9] However, all the structures reported so far have been governed by the geometrical packing of surfactants[4, 10] because the formation of the mesostructured precursors relies on the cooperative organization of inorganic species and surfactants.[11] Herein, we report on the formation of novel mesoporous silicas (denoted as KSW-2) with rectangular arrangements of square or lozenge one-dimensional (1D) channels by mild acid treatment of a layered alkyltrimethylammonium (C_nTMA)–kanemite complex. Mesostructured precursors of KSW-2 formed through the bending of individual silicate sheets of kanemite. The square or lozenge shape of the relatively ordered pores has not previously been found among the reported mesoporous and mesostructured inorganic oxides.

Kanemite ($NaHSi_2O_5 \cdot 3H_2O$), a mineral, is made up of layered polysilicates composed of SiO_4 tetrahedral units,[12] and the crystal structure was recently determined by Gies et al.[13] Kanemite is a layered silicate composed of single sheets such as δ-$Na_2Si_2O_5$ and $KHSi_2O_5$; the sheets are constructed by connecting 6-rings of SiO_4 tetrahedra wrinkled

[*] Prof. Dr. K. Kuroda,[+] Dr. T. Kimura, T. Kamata, Y. Takano, Prof. Dr. Y. Sugahara
Department of Applied Chemistry, Waseda University
Ohkubo 3-4-1, Shinjuku-ku, Tokyo 169-8555 (Japan)
Fax: (+81) 3-5286-3199
E-mail: kuroda@mn.waseda.ac.jp

[+] Kagami Memorial Laboratory for Materials Science and Technology
Waseda University, Nishiwaseda 2-8-26, Shinjuku-ku, Tokyo 169-0051 (Japan)

M. Fuziwara
Materials Characterization Central Laboratory, Waseda University
Ohkubo 3-4-1, Shinjuku-ku, Tokyo 169-8555 (Japan)

M. Kaneda, Dr. Y. Sakamoto, Prof. Dr. O. Terasaki
Department of Physics, Graduate School of Science
Tohoku University, Sendai, 980-8578 (Japan)

Prof. Dr. O. Terasaki
CREST, JST and Center for Interdisciplinary Research
Tohoku University, Sendai, 980-8578 (Japan)

[**] This work was supported by CREST, Japan Science and Technology Corporation, and Grant-in-Aid for the Scientific Research from the Ministry of Education, Science, Sports, and Culture of the Japanese Government.

Supporting information for this article is available on the WWW under http://www.wiley-vch.de/home/angewandte/ or from the author.

  1433-7851/00/3921-3855 $ 17.50+.50/0

regularly with interlayer hydrated Na^+ ions.[13, 14] Following the report on the synthesis and reactivity of kanemite by Beneke and Lagaly,[15] Yanagisawa et al. discovered a mesoporous silica (named as KSW-1 hereafter) by the reaction of kanemite and C_nTMA surfactants.[1]

A mesostructured precursor of KSW-2 was obtained from a layered C_{16}TMA–kanemite complex by adjusting the pH value below 6.0. The preparation of the layered complex without altering the structure of the silicate framework is the most important step in obtaining the mesostructured precursor. Therefore, the synthesis procedure for KSW-2 is quite different from those reported for KSW-1 and FSM-16 derived from kanemite.[1, 16]

A typical transmission electron microscopy (TEM) image and the corresponding electron diffraction (ED) pattern of the calcined KSW-2 obtained under the adjusted pH value of 4.0 are shown in Figure 1 a. The TEM image of the calcined

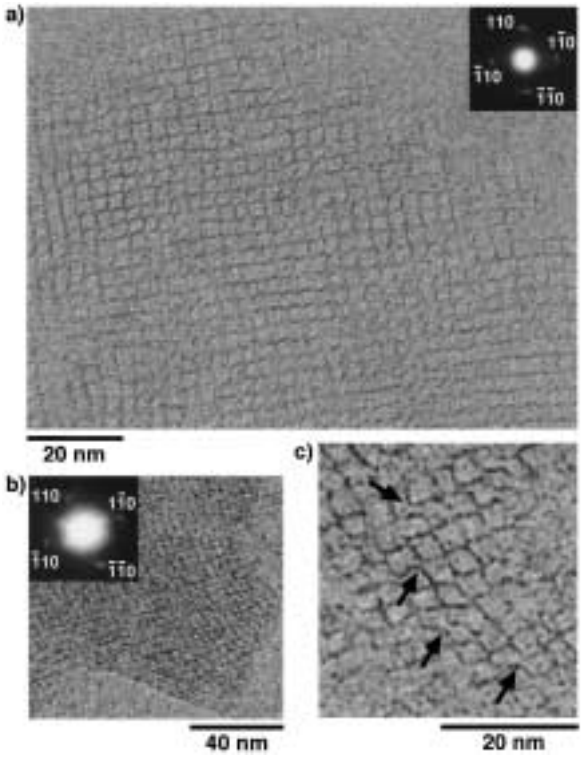

Figure 1. a) Typical TEM of calcined KSW-2 (pH 4.0) and the corresponding ED pattern indexed as *hk0* projection. These were obtained by a JEM-3010 transmission electron microscope operated at 300 kV. b) Typical TEM and the corresponding ED pattern of as-synthesized KSW-2 (pH 6.0). c) Another TEM of the as-synthesized KSW-2 (pH 6.0). Arrows imply the observed place of the bending of silicate sheets derived from kanemite.

KSW-2 exhibits relatively ordered square arrangements that display a periodic distance of adjacent pores of about 3.3 nm. Striped patterns with the same periodic distance were also observed, strongly supporting the presence of one-dimensional (1D) mesopores. The ED pattern showed the angle of diagonal lines connecting the [110] spots was close to 90°.

On the basis of the TEM results, all the powder X-ray diffraction (XRD) peaks of the as-synthesized and calcined KSW-2 are assigned to an orthorhombic structure (*C2mm*) (as-synthesized: $a = 5.34$ nm, $b = 5.05$ nm, $c = \infty$; calcined: $a = 4.84$ nm, $b = 4.26$ nm, $c = \infty$; Figure 2).[*] After calcination, the d_{110} value changed from 3.67 nm to 3.26 nm, which is in agreement with the periodic distance of adjacent pores observed by TEM (ca. 3.3 nm). On the basis of the N_2 adsorption isotherm of the calcined KSW-2, the BET surface area, the pore volume, and the average pore diameter were determined to be $1100\ m^2 g^{-1}$, $0.46\ cm^3 g^{-1}$, and 2.1 nm, respectively.[17]

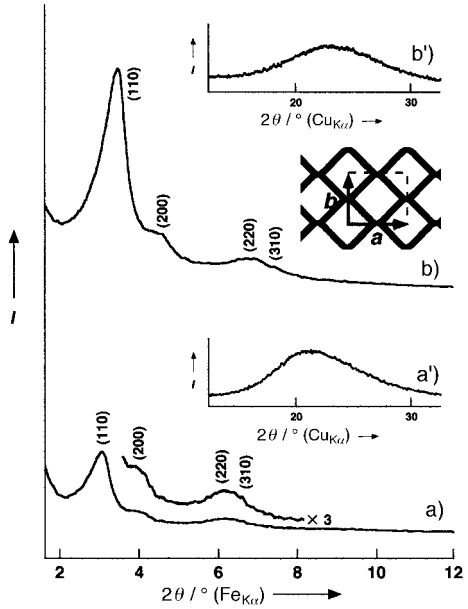

Figure 2. Powder XRD patterns of KSW-2 materials prepared at pH 4.0 a) before and b) after calcination. These were recorded by a Mac Science M03XHF[22] diffractometer with monochromated $Fe_{K\alpha}$ radiation. a′), b′) XRD patterns in higher 2θ regions were obtained by a Mac Science MXP[3] diffractometer with monochromated $Cu_{K\alpha}$ radiation.

The mesopores are surrounded by relatively flat silicate walls (Figure 1 a). Typical scanning electron micrographs showed that all the products have not morphologically changed; all the images are similar to that of kanemite (see Supporting Information, Figure A). This indicates that kanemite did not dissolve during the syntheses of both the layered C_{16}TMA–kanemite complex and the as-synthesized KSW-2, because the reactions were conducted at relatively low pH values at which silica does not dissolve.[12]

Square-shaped mesopores have not been found among the reported ordered mesoporous materials[1-11, 16] because those mesostructures were constructed by using supramolecular assemblies and were thus governed by their geometries.[4, 10] Although the transformation of lamellar mesophase silicates has been conducted by hydrothermal post treatment[18] or acid treatment,[19] these types of transformation occur through the rearrangement of silicate frameworks and lead to the formation of hexagonal and cubic mesophase silicates, in which the silicate walls are formed along the curved surface of organic assemblies such as rodlike micelles. Even for KSW-1 and FSM-16, which were prepared by the direct reactions of

[*] We observed that the structural units of kanemite are partly retained, as discussed later, and therefore chose a 3D representation rather than a 2D one.

  1433-7851/00/3921-3856 $ 17.50+.50/0 *Angew. Chem. Int. Ed.* **2000**, *39*, No. 21

kanemite and C_nTMA surfactants,[1, 15] the resulting mesostructure is hexagonal or less ordered.

The samples were prepared at various adjusted pH values above 4.0 in order to investigate the formation mechanism of the as-synthesized KSW-2. The ^{29}Si MAS NMR spectra of kanemite, the layered C_{16}TMA–kanemite complex, and the acid-treated products are shown in Figure 3. The spectrum of kanemite exhibited only one peak at $\delta = -97$, indicating that

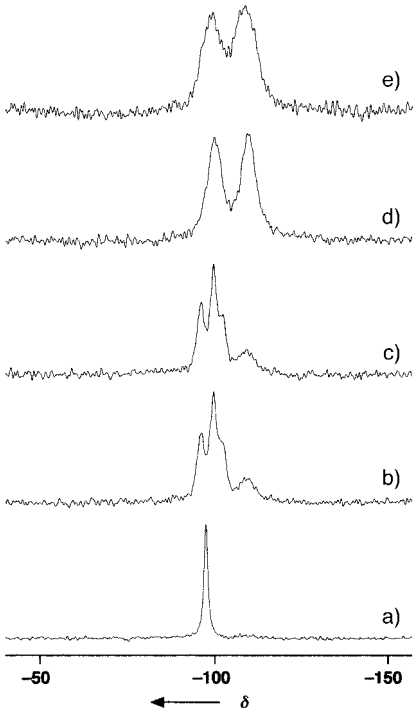

Figure 3. ^{29}Si MAS NMR spectra of a) kanemite, b) layered C_{16}TMA–kanemite complex, and c)–e) the products treated with acetic acid to give pH values of 8 (c), 6 (d), and 4 (e). These were obtained by a JEOL GSX-400 spectrometer with a spinning rate of 5 kHz and a resonance frequency of 79.30 MHz with a 45° pulse length of 4.1 μs and a recycle time of 60 s. The chemical shifts were expressed with respect to tetramethylsilane.

kanemite is composed of single-layered silicate sheets (Figure 3a).[13, 14] In the spectrum of the layered C_{16}TMA–kanemite complex several peaks due to different Q^3 environments ($(SiO)_3SiO$) were mainly observed in the range from $\delta = -95$ to -105,[12] whereas a broad peak centered at $\delta = -110$ due to a Q^4 environment ($(SiO)_3SiOSi$) was detected as a minor component (Figure 3b). This result reveals that the single silicate sheet structure in kanemite was essentially retained during the synthesis of the layered C_{16}TMA–kanemite complex. At a pH value of 8.0, the spectrum of the product hardly changed and the peak intensity at $\delta = -110$ increased slightly (Figure 3c). In contrast, the profiles of the acid-treated products obtained at pH values below 6.0 varied dramatically (Figure 3d, e); both the Q^3 and Q^4 peaks centered at $\delta = -101$ and -110, respectively, were observed, which is in accordance with the structural change from the layered C_{16}TMA–kanemite complex to the as-synthesized KSW-2.

The as-synthesized product was thoroughly investigated by high-resolution TEM (HRTEM) at the point at which the structural change occurs (pH 6.0). As well as the TEM images observed for calcined KSW-2 (pH 4.0), similar images were observed and the periodic distance between adjacent pores was about 4.0 nm (Figure 1b); the angle of diagonal lines connecting the [110] spots was variable, ranging from nearly 90° to about 70° in the ED patterns. It was not possible to superimpose the striped patterns because the angle of the diagonal lines falls in a limited range (70–90°) and the images were observed at thin parts of the sample.

The bending of individual silicate sheets, which are not fully linked between adjacent layers, was partly observed (see Figure 1c). This observation is reproducible; the bending was directly observed by HRTEM for KSW-2 synthesized in another batch (see Supporting Information, Figure B). In addition, the range of pH values during the acid treatment did not lead to dissolution of silicate species, but led to their condensation.[12] The observed wall thicknesses of the products during the acid treatment were almost constant (0.6–0.7 nm), and were consistent with the thickness of the silicate sheet in kanemite.[13, 14] These findings strongly suggest that as-synthesized KSW-2 can be obtained from the layered C_{16}TMA–kanemite by bending the individual silicate sheets. Even in the TEM image of calcined KSW-2 (pH 4.0), bent silicate sheets were observed to a certain extent (Figure 1a).

The variations in C,H,N analysis (C_{16}TMA/Si ratio) and ^{29}Si MAS NMR spectra ($Q^4/(Q^3+Q^4)$ ratio) of the products during the acid treatment are shown in Figure 4. On the basis of this data, the transformation steps of the layered complex into as-synthesized KSW-2 are schematically shown in Figure 5 and can be categorized as follows. 1) The $Q^4/(Q^3+Q^4)$ ratio increases in the range of pH 9.6–7.0, and C_{16}TMA/Si ratio decreases slightly. This observation suggests that the beginning of the structural change is manifested by the formation of Q^4 silicate species. The formation of Q^4 species

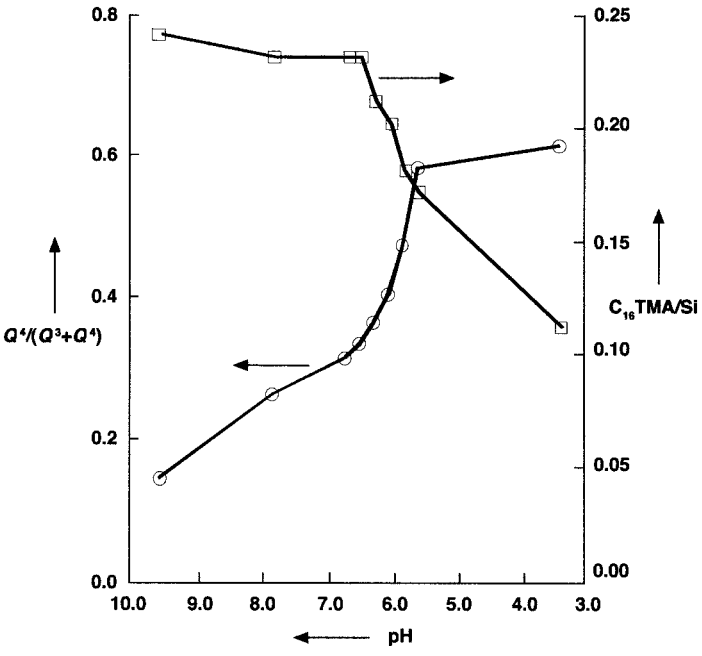

Figure 4. Variation in the amounts of C_{16}TMA ions and the $Q^4/(Q^3+Q^4)$ ratios during acid treatment. The organic contents for calculation of C_{16}TMA/Si ratios of the acid-treated products were obtained with a Perkin Elmer PE-2400II.

  1433-7851/00/3921-3857 $ 17.50+.50/0

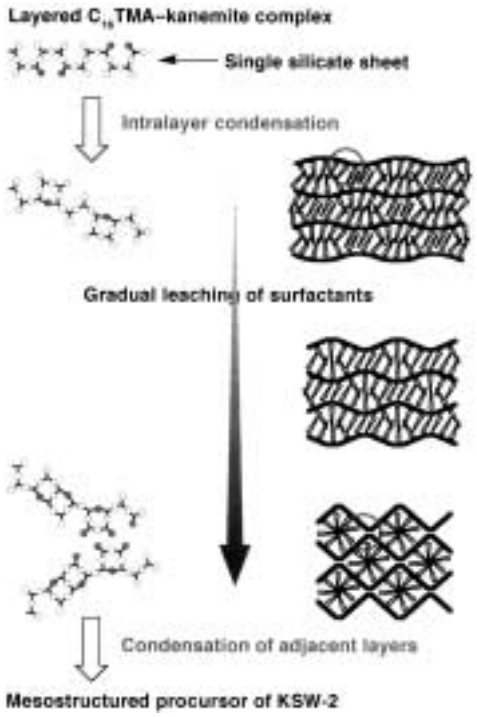

Figure 5. Schematic model for the formation of as-synthesized KSW-2 from a layered C_{16}TMA – kanemite complex. Oxygen atoms are denoted by open circles; those involved in the structural change are filled. On the basis of the schematic structure of kanemite, adjacent Si–OH groups are in very close proximity. Although the reaction steps are distinguished for convenience, these steps progress cooperatively.

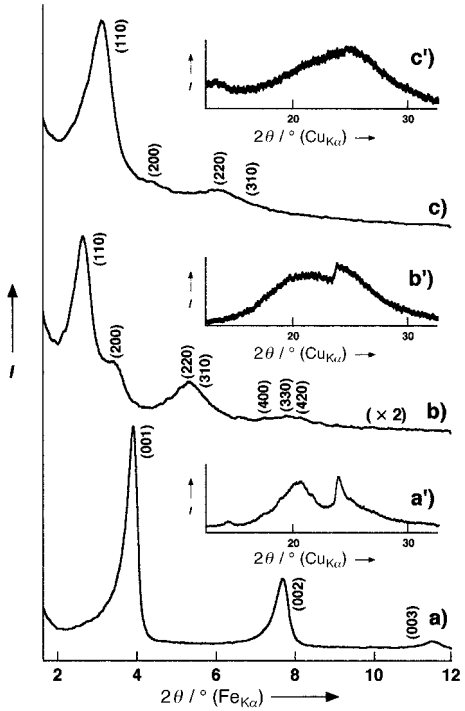

Figure 6. Powder XRD patterns of a layered C_{16}TMA – kanemite complex (a) and KSW-2 materials prepared at pH 6.0 before (b) and after calcination (c). These patterns including a′) – c′) were recorded by the same procedure as in Figure 2. For the layered C_{16}TMA – kanemite complex, the broad peak centered at $2\theta = 21.1^\circ$ seems to be overlapped by several peaks.

occurs at the intralayers, since the structural change at pH 8.0 was hardly visible by XRD (see Supporting Information, Figure C). 2) In the range of pH 7.0 – 6.0, the transformation of the layered complex into as-synthesized KSW-2 is caused by partial removal of C_{16}TMA ions. The $Q^4/(Q^3 + Q^4)$ ratio increases further, indicating the condensation between adjacent layers as well as progressive intralayer condensation. 3) In the structural change at pH values below 6.0, additional condensation among Q^3 silicate species occurs between the adjacent layers. KSW-2 with a square 1D arrangement is thought to be formed through these processes (Figure 5).

The layered silicate network originating from the structure of kanemite connects two-dimensionally and is not destroyed under the conditions used. Thus, the bending of individual silicate sheets may be attributed to the limited structural changes that result from partial intralayer condensation and the accompanying structural change in C_{16}TMA assemblies during the gradual leaching. The crystal structure of kanemite,[13, 14] reveals the intralayer condensation of Si–OH groups is possible only in the limiting direction. Indeed, the angles between the silicate sheets (after bending) and the edge of kanemite particles, observed by TEM, were often been around 45° (Figure 1 a; see also Supporting Information, Figure B).

The XRD patterns of the as-synthesized and the calcined products (pH 6.0) are shown in Figure 6. As in the case with the products obtained at pH 4.0, all the peaks at low 2θ angles are assigned to an orthorhombic structure (as-synthesized: $a = 6.34$ nm, $b = 5.58$ nm, $c = \infty$; calcined: $a = 5.16$ nm, $b =$ 4.92 nm, $c = \infty$). Interestingly, the XRD profiles in the range 15° to 30° are somewhat different from those observed for the mesoporous materials reported up to date.[1–11, 16, 18, 19] Though halo XRD peaks were observed for the KSW-2 materials obtained at pH 4.0 (see Figures 2 a′ and b′), the XRD patterns of the KSW-2 materials prepared at pH 6.0 showed somewhat unusual peaks in the range 15° to 30°. The XRD pattern of the layered C_{16}TMA – kanemite complex (Figure 6 a′) at higher angles showed a broad peak centered at $2\theta = 21.1^\circ$ and a sharp one at 24.3°, suggesting that the structural units of kanemite are at least partly retained in the layered C_{16}TMA – kanemite complex. Even in as-synthesized KSW-2, these peaks remained with some broadening (Figure 6 b). Although further broadening of such peaks was observed after calcination at 550 °C for 6 h, the profile in the range of 15° to 30° was somewhat different from those observed for the mesoporous materials reported so far.[1–11, 16, 18, 19] Further characterization of the structural features is currently in progress. On the basis of the N_2 adsorption isotherm, the BET surface area, the pore volume, and the average pore diameter of the calcined product were determined to be 1192 $m^2 g^{-1}$, 0.56 $cm^3 g^{-1}$, and 2.8 nm, respectively. The material has a high hydrocarbon sorption capacity on the basis of an adsorbed amount of benzene (0.74 $g g^{-1}$ at $P/P_0 = 0.65$).

We utilized a layered C_{16}TMA – kanemite complex as the starting material, in which the basic structural framework was retained at least partly after the formation of the layered complex. The formation mechanism of KSW-2 proposed here is based on the bending of intralayer-condensed silicate sheets

  1433-7851/00/3921-3858 $ 17.50+.50/0

of kanemite. The resulting square pore system has not been observed among reported mesoporous materials[1–11, 16, 18, 19] and is not defined by the geometrical packing of surfactant molecules.[4, 10] Although the frameworks are not fully retained after calcination, this approach provides a way to incorporate inorganic structural units into mesostructured materials, which will lead to the development of novel mesoporous materials with crystalline inorganic frameworks.

Experimental Section

A layered C_{16}TMA–kanemite complex was prepared by mixing a layered polysilicate kanemite ($NaHSi_2O_5 \cdot 3H_2O$ (1.05 g) derived from δ-$Na_2Si_2O_5$ (1.00 g)) and a 0.1 M C_{16}TMACl aqueous solution (200 mL) at room temperature; the C_{16}TMA/Si ratio was 2. The resulting C_{16}TMA–kanemite complex is a layered material, which was confirmed by the powder XRD pattern of the product (Figure 6a). The peak at a *d* spacing of 2.9 nm and the higher ordered diffraction peaks were observed, and the spacings increased when *n*-decyl alcohol was further intercalated into the product. The resulting layered complex (1.01 g) was dispersed in distilled water (150 mL; pH ca. 9.6). The pH value of this suspension was decreased by the addition of acetic acid (1 M); the addition procedure was conducted slowly over 30 min. The as-synthesized KSW-2 powders were air-dried and calcined at 550 °C with a heating rate of 10 K min^{-1} in ambient air for 6 h to remove organic fractions. Although the acid species are not significant for the synthesis of KSW-2, the concentration of acids must be carefully chosen, depending on the acid species used. The amount of distilled water and the adjusted pH value are also important because the solubility of C_nTMA ions is one of the key conditions for the formation of KSW-2.

Received: March 2, 2000
Revised: June 17, 2000 [Z14796]

[1] T. Yanagisawa, T. Shimizu, K. Kuroda, C. Kato, *Bull. Chem. Soc. Jpn.* **1990**, *63*, 988–992.
[2] C. T. Kresge, M. E. Leonowicz, W. J. Roth, J. C. Vartuli, J. S. Beck, *Nature* **1992**, *359*, 710–712.
[3] Q. Huo, D. I. Margolese, U. Ciesla, P. Feng, T. E. Gler, P. Sieger, R. Leon, P. M. Petroff, F. Schüth, G. D. Stucky, *Nature* **1994**, *368*, 317–321.
[4] Q. Huo, R. Leon, P. M. Petroff, G. D. Stucky, *Science* **1995**, *268*, 1324–1327.
[5] A. Corma, *Chem. Rev.* **1997**, *97*, 2373–2419.
[6] H. Yang, A. Kuperman, N. Coombs, S. Mamiche-Afara, G. A. Ozin, *Nature* **1996**, *379*, 703–705; H. Yang, N. Coombs, I. Sokolov, G. A. Ozin, *Nature* **1996**, *381*, 589–592.
[7] Y. Lu, R. Ganguli, C. A. Drewien, M. T. Anderson, C. J. Brinker, W. Gong, Y. Guo, H. Soyez, B. Dunn, M. H. Huang, J. I. Zink, *Nature* **1997**, *389*, 364–368.
[8] A. Sayari, P. Liu, *Microporous Mater.* **1997**, *12*, 149–177.
[9] T. Kimura, Y. Sugahara, K. Kuroda, *Chem. Lett.* **1997**, 983–984; T. Kimura, Y. Sugahara, K. Kuroda, *Chem. Commun.* **1998**, 559–550; T. Kimura, Y. Sugahara, K. Kuroda, *Microporous Mesoporous Mater.* **1998**, *22*, 115–126; T. Kimura, Y. Sugahara, K. Kuroda, *Chem. Mater.* **1999**, *11*, 508–518.
[10] Q. Huo, D. I. Margolese, G. D. Stucky, *Chem. Mater.* **1996**, *8*, 1147–1160.
[11] A. Firouzi, D. Kumar, L. M. Bull, T. Besier, P. Sieger, Q. Huo, S. A. Walker, J. A. Zasadzinski, C. Glinka, J. Nicol, D. Margolese, G. D. Stucky, B. F. Chmelka, *Science* **1995**, *267*, 1138–1143.
[12] F. Liebau, *Structural Chemistry of Silicates*, Springer, Heidelberg, **1985**, and the references therein. The variation in the chemical shifts is probably due to the changes in the various bond angles among SiO_4 tetrahedra in the single layered silicate sheets owing to the difference in the ionic radii between Na^+ and the head group of $C_{16}TMA^+$.
[13] H. Gies, B. Marler, S. Vortmann, U. Oberhagemann, P. Bayat, K. Krink, J. Rius, I. Wolf, C. Fyfe, *Microporous Mesoporous Mater.* **1998**, *21*, 183–197; S. Vortmann, J. Rius, B. Marler, H. Gies, *Eur. J. Mineral.* **1999**, *11*, 125–134.
[14] L. A. J. Garvie, B. Devouard, T. L. Groy, F. Camara, P. R. Buseck, *Am. Mineral.* **1999**, *84*, 1170–1175.
[15] K. Beneke, G. Lagaly, *Am. Mineral.* **1977**, *62*, 763–771.
[16] S. Inagaki, A. Koiwai, N. Suzuki, Y. Fukushima, K. Kuroda, *Bull. Chem. Soc. Jpn.* **1996**, *69*, 1449–1457. The obtained mesoporous silica in the paper was denoted as FSM-16.
[17] G. Horváth, K. Kawazoe, *J. Chem. Eng. Jpn.* **1983**, *16*, 470–475. The pore size was calculated from the adsorption branch by the Horváth–Kawazoe method.
[18] A. Monnier, F. Schüth, Q. Huo, D. Kumar, D. Margolese, R. S. Maxwell, G. D. Stucky, M. Krishnamurty, P. Petroff, A. Firouzi, M. Janicke, B. F. Chmelka, *Science* **1993**, *261*, 1299–1303.
[19] C. A. Fyfe, G. Fu, *J. Am. Chem. Soc.* **1995**, *117*, 9709–9714.

Second-Order Nonlinear Optical Properties of Functionalized Ionophores: Cation-Steered Modulation of the First Hyperpolarizability**

Stephan Houbrechts,* Yuji Kubo, Tomokazu Tozawa, Sumio Tokita, Tatsuo Wada,* and Hiroyuki Sasabe

Functionalized ionophores are of major interest for their ability to complex various ionic species. As complex formation generally induces severe changes in their photophysical properties, they are widely used as a tool for ion recognition. Accordingly, the influence of cation binding on the intramolecular charge-transfer (ICT) transition has been studied intensively, mostly on donor–acceptor substituted aromatic chromoionophores.[1–3] Among them, two classes of ionophores can be distinguished (Scheme 1): type A chromophores that interact with the ion through the acceptor site of the chromophore, which enhances the ICT and induces a bathochromic shift of the charge transfer band; and type B chromophores that interact via the donor site and reduce the ICT (hypsochromic shift).

[*] Dr. S. Houbrechts,[+] Dr. T. Wada, Dr. H. Sasabe
Frontier Research Program
The Institute of Physical and Chemical Research (RIKEN)
2-1 Hirosawa, Wako, Saitama 351-01 (Japan)
Fax: (+49) 48-462-4695
E-mail: stephan.houbrechts@fys.kuleuven.ac.be, tatsuow@postman.riken.go.jp
Prof. Dr. Y. Kubo
Form and Function, PRESTO
Japan Science and Technology Corporation (JST)
Department of Applied Chemistry
Saitama University
255 Shimo-ohkubo, Urawa, Saitama 338-8570 (Japan)
Prof. Dr. Y. Kubo, T. Tozawa, Prof. Dr. S. Tokita
Department of Applied Chemistry
Saitama University
255 Shimo-ohkubo, Urawa, Saitama 338-8570 (Japan)
[+] Present address:
Laboratory of Chemical and Biological Dynamics
Catholic University of Leuven
Celestijnenlaan 200D, 3001 Heverlee (Belgium)
Fax: (+32) 16-327982

[**] This work was supported by the Frontier Research Program and the Japan Science and Technology Corporation. S.H. is a postdoctoral researcher of the FWO (Flanders).